BMC Chemistry

RESEARCH

Open Access

Isolation of highly polar galloyl glucoside tautomers from *Saxifraga tangutica* through preparative chromatography and assessment of their in vitro antioxidant activity

Yingying Tong[1,2], Ming Chu[2], Jia Zhou[1,2], Qilan Wang[1], Gang Li[2], A. M. Abd El-Aty[3,4] and Jun Dang[1*]

Abstract

In this work, the rapid and efficient preparation of isolated galloyl glucoside tautomer free radical inhibitors was investigated using *Saxifraga tangutica* as a raw material. Four highly polar galloyl glucoside tautomers, 3-*O*-galloyl-α-D-glucose ⇌ 3-*O*-galloyl-β-D-glucose (Fr2-1-1), 2-*O*-galloyl-α-D-glucose ⇌ 2-*O*-galloyl-β-D-glucose (Fr2-1-2/2-1-3), 1-*O*-galloyl-β-D-glucose (Fr2-2-1), and 6-*O*-galloyl-α-D-glucose ⇌ 6-*O*-galloyl-β-D-glucose (Fr2-3-1/Fr2-3-2), were obtained via two-step medium-pressure liquid chromatography (with solid loading instead of conventional liquid injection) and one-step high-performance chromatography coupled with on-line RPLC-DPPH techniques for targeted isolation. This separation integration technique not only increases sample intake and reduces time cost but also visualizes each step of targeted separation. All four compounds were isolated from the plant for the first time. In vitro antioxidant activity assays by DPPH (1,1-diphenyl-2-picrylhydrazyl) revealed that Fr2-1-2/Fr2-1-3 (IC_{50}: 5.52 ± 0.32 μM), Fr2-2-1 (IC_{50}: 7.22 ± 0.57 μM), and Fr2-3–1/Fr2-3-2 (IC_{50}: 7.36 ± 0.25 μM) had superior free radical scavenging abilities and that both were superior to that of quercetin (IC_{50}: 18.61 ± 3.55 μM). Oxidative stress assays revealed that Fr2-1-2/Fr2-1-3 significantly inhibited oxidative stress damage in H_2O_2-induced HepG2 cells, decreased the level of ROS ($P < 0.01$) and protected hepatocytes. Combined with the current results, gallic acid showed greater antioxidant activity when H atoms were replaced at D-glucose –OH (C-2) than at the other three sites [–OH (C-1), –OH (C-6) and –OH (C-3)].

Keywords *Saxifraga tangutica*, Isolation, Galloyl glucoside tautomers, Antioxidative activity, HepG2 cells, Structure–activity relationships

*Correspondence:
Jun Dang
dangjun@nwipb.cas.cn
Full list of author information is available at the end of the article

Introduction

The disharmony between oxidant and antioxidant chemicals and the accumulation of reactive oxygen species (ROS) and reactive nitrogen species (RNS) in cells and organs lead to oxidative stress, resulting in oxidative damage to cellular macromolecules in the body [1]. An imbalance of oxidation and antioxidant activity in the body is thought to be a vital ingredient in aging and disease [2]. In the northern hemisphere, where nearly 90% of the global population lives, autumn and winter are periods of high incidence of respiratory diseases [3]. Oxidative stress in respiratory diseases is a major concern [4]. Japanese microbiologist Akaike et al., circa 1990, reported that the real pathologic factor directly contributing to pneumonia and multiorgan injury caused by respiratory virus infection is the presence of excess active free radicals and active nitrogen free radicals [5]. The inflammatory cytokine storm caused by an overactive immune response induced by infection is one of the direct pathologic factors of the ROS molecular storm [6]. In addition, oxidative stress levels are increased under hypoxic conditions [7]. Free radical inhibitors are important tools for preventing and delaying these diseases [8–10]. Currently, many drugs have been developed on the basis of the regulation of oxidative stress [11]. In general, oxidative stress is an area of concern. Therefore, one of the new ways to find cures for diseases is to look for antioxidants or other pharmacological drugs that act as antioxidants and strengthen the body's antioxidant defense.

Saxifraga tangutica (*S. tangutica*), a genus of Saxifrage in the Saxifrage family, is an herbaceous perennial found at high altitudes (2900–5600 m). It has a strong, slightly bitter flavor. Both traditional and contemporary medicine use it extensively to treat liver and gallbladder fever, trauma, and gastrointestinal issues [12]. *S. tangutica* contains a broad range of chemicals, including steroids, diarylheptanes, phenols, flavonoids, and phenylpropanoids [13, 14]. To date, a component activity-oriented approach has been used to isolate eight antioxidant phenols from *S. tangutica*: protocatechuic aldehyde, ethyl gallate, rhododendron, *p*-hydroxyphenethylphenol, ethyl protocatechuic acid, *o*-aminophenone, and ethyl *p*-benzoate [15, 16].

Considerable time and spirit are needed to separate antioxidants from natural products (NPs) via traditional separation techniques [17]. Following each stage of separation, the antioxidant capacity needs to be determined. The process of separating chemicals from complicated natural extracts is intricate and requires specialized methods [18]. Thus, designing an accurate and quick analysis-targeted separation-efficient separation and analysis approach for the preparation and purification of additional antioxidants is imperative. Furthermore, research on the biological activities that follow the isolation of antioxidants from other natural products is highly important. With the notable benefit of integrating the separation and identification of antioxidant active components or compounds, this online high-performance liquid chromatography-1,1-diphenyl-2-picrylhydrazyl (HPLC-DPPH) bioassay-guided analysis approach for the identification of antioxidant chemicals in NPs satisfies this demand.

In previous studies, the authors developed several online HPLC-DPPH systems to identify and combine them with high resolution electrospray ionization-mass spectrometry (ESI-HRMS) systems (HPLC-DPPH) to identify antioxidants in NPs [19]. The aim of this study was to enable online reversed-phase liquid chromatography (RPLC)-DPPH analysis combined with RPLC identification, isolation, purification and characterization of galloyl glucoside tautomer free radical inhibitors from *S. tangutica*. This is the first isolation and purification of galloyl glucoside tautomer radical inhibitors from NPs. Additionally, we assessed the antioxidant activity of these compounds in vitro and explored the conformational relationships of these compounds. Moreover, the intervention of H_2O_2-induced oxidative stress injury in HepG2 cells by these compounds confirmed the protective effect of galloyl glucoside tautomer free radical inhibitors against oxidative stress injury in HepG2 cells. These findings provide an experimental basis and theoretical basis for further mechanistic studies. The activity-directed online targeted isolation technique provides new ideas and insights for the efficient isolation of free radical inhibitors from other NPs.

Materials and methods

Chemicals and reagents

HPLC-grade methanol (MeOH) and acetonitrile (ACN) used for HPLC analysis were obtained from Shanxi Xian SHUNDA Chemical Reagent Instrument. MeOH, ACN, and ethanol (EtOH) of analytical grade were obtained from Zhengzhou Paini Chemical Reagent Factory (Henan, China). HPLC-grade water was produced through a Moore water system (Chongqing, China). Formic acid (FA) was purchased from Shanghai McLean Biochemical Technology Co (China). Dulbecco's modified Eagle's medium (DMEM), fetal bovine serum (FBS) and trypsin–EDTA solution were obtained from Gibco (Carlsbad, CA, USA). 3-(4,5-dimethylthiazol-2-thiazolyl)-2,5-diphenyltetrazolium bromide (MTT), 2,7-dichlorodi-hydrofluorescein diacetate (DCFH-DA), dimethylsulfoxide (DMSO), quercetin (QR) and DPPH were purchased from Sigma–Aldrich, Steinheim.

Equipment

Sample pretreatment was performed on a Hanbon preparative HPLC unit: with a UV–Vis detector, three pumps and an EasyChorm workstation. Online HPLC-DPPH testing was performed using an Essential LC-16 instrument and an LC-10AD instrument (Shimadzu Corporation, Japan). The two components are functionally distinct and include efficient separation (LC-16) and DPPH-binding activities (LC-10AD). The separation system (LC-16) consists of two LC-16 pumps, one SPD-16 detector, one SIL-16 automatic sampler, one DGU-20A degassing unit, one external column incubator and a LabSolutions workstation. The activity screening system (LC-10AD) screens for DPPH free radical activity via an LC-10AD pump, a PDA detector and a LabSolutions workstation.

Stationary phases

The separation of *S. tangutica* was performed on three commercial stationary phases, including MCI GEL® CHP20P (120 μm, Mitsubishi Chemical Corporation, Japan), Spherical C18 (50 μm, Greenherbs Science & Technology, China) and ReproSil-Pur C18 AQ (4.6×250 mm and 20×250 mm, 5 μm, SapoRex Beijing Science & Technology Corporation, China).

Plant and cell

Saxifraga tangutica samples were collected at an altitude of 4520 m (August 2016) from Guoluo, Qinghai, China (34° 33′ 37.08″ N, 99° 47′ 35.16″ E). Prof. Lijuan Mei (Northwest Institute of Plateau Biology, Chinese Academy of Sciences) identified the sample, and a sample (No. 0325734) for *S. tangutica* was held at the Qinghai-Tibetan Plateau Museum of Biology. The HepG2 cell line was obtained from Shanghai Hongshun Biotechnology Co. (China).

Extraction and preparation of the *Saxifraga tangutica* Fr2 sample

Dried and ground *S. tangutica* (500 g) herbs were extracted with MeOH (three times, 4.0 L once) at room temperature. The total extract solutions (12.0 L) were concentrated to the decompression state in a thermostatic water bath (40 °C). Approximately 300.0 mL of the crude extract was obtained. First, 200.0 g of polyamide was weighed, mixed with curde extract and subsequently dried in an oven at 40 °C. The dried mixture was loaded via a small medium-pressure column (22.0 g per loading, total weight of the mixture was 265.0 g), and the samples were enriched in the head of a pretreatment column (stationary phase: MCI GEL® CHP20P, 49×460 mm) and separated by elution. The gradient elution conditions were as follows: 1) 0–120 min, 0%–100% EtOH; 2) 120–150 min, 100% EtOH) at a 30.0 mL/min flow rate. Chromatograms were obtained at 254 nm. Six fractions (Fr1–Fr6) were obtained after 12 repetitions of pretreatment, of which the target fraction Fr2 (2.84 g) was used for subsequent separation.

DPPH inhibitor recognition, separation and activity assessment of the *Saxifraga tangutica* Fr2 sample

Activity screening of Fr2 was performed via the online RPLC-DPPH method. The adsorbent stationary phase was ReproSil-Pur C18 AQ, with a stationary phase particle size of 5 μm. The mobile phases were HPLC-grade H_2O (containing 0.2% FA *v/v*, solution A) and HPLC-grade ACN (solution B). Briefly, the Fr2 obtained from the treatment was redissolved in 50.0 mL of 50% MeOH/H_2O (*v/v*) and percolated through an organic membrane (0.22 μm). Fr2 was then chromatographed on an LC-16 system using ReproSil-Pur C18 AQ. A gradient elution mode was used to elute at a flow rate (1.0 mL/min) that allowed 0% B to increase linearly to 22% B within 60 min under analytical conditions (injection volume of 5.0 μL), and the column oven temperature was fixed at 30 °C. Subsequently, access to the LC-10AD system was achieved, and the active ingredient was monitored at 517 nm via a DPPH (25 μg/mL) ethanol solution at a flow rate of 0.8 mL/min.

Separation was carried out for RPLC-DPPH-screened Fr2 on a Spherical C18 stationary phase using the same mobile phase as the analytical conditions. The elution program was as follows: 0–80 min, 5%–50% B. The injection was repeated 5 times (each injection volume of 10.0 mL) at a flow rate of 70.0 mL/min, and the detection wavelength was the same as that used pretreatment (254 nm).

The three fractions (Fr2-1 199.1 mg, Fr2-2 749.4 mg and Fr2-3 255.8 mg) obtained from the Sphercial C18 stationary phase were further separated on a ReproSil-Pur C18 AQ column. The solutions of pump A and pump B for Fr2-1 were HPLC-grade H_2O (containing 0.2% FA *v/v*) and HPLC-grade ACN, respectively. The compositions of the solutions of Fr2-2 and Fr2-3 were the same as that of Fr2-1. The elution programs for Fr2-1 (50% MeOH in H_2O (*v/v*), dissolution volume of 4.0 mL), Fr2-2 (50% MeOH in H_2O (*v/v*), dissolution volume of 10.0 mL), and Fr2-3 (50% MeOH in H_2O (*v/v*), dissolution volume of 10.0 mL) were as follows: (1) 0–30 min, 0%–6% B, injection volume of 1.0 mL; (2) 0–30 min, 1%–4% B, injection volume of 1.5 mL; and (3) 0–30 min, 3%–6% B, injection volume of 1.5 mL. Chromatograms were recorded at 254 nm.

The antioxidant activities of the isolated compounds (Fr2-1-1, Fr2-1-2/Fr2-1-3, Fr2-2-1 and Fr2-3-1/Fr2-3-2)

were evaluated on a ReproSil-Pur C18 AQ column with an online RPLC-DPPH system. The mobile phase and detection wavelength were the same as those used for the isolation of Fr2-1. Isocratic elution mode was used for Fr2-1-1, Fr2-1-2/Fr2-1-3, Fr2-2-1 and Fr2-3-1/Fr2-3-2, with elution steps of 0% B (0–30 min), 1% B (0–30 min), 1% B (0–30 min) and 3% B (0–30 min), respectively. The column oven temperature was set to 30 °C in all the cases. The concentration, flow velocity and detection wavelength of DPPH in the LC-10AD system were the same as before.

Determination of DPPH free radical clearance ability

The DPPH radical scavenging activities of the compounds and QR (QR was used as a positive control) at different concentrations were determined according to the methods of Feng et al. [20]. DPPH (1.0 mg) was accurately weighed, dissolved in 40.0 mL of 50% EtOH/H_2O (*v/v*) (25 mg/L), and preserved under light-avoidance conditions (0–4 °C). Both the compounds and QR were dissolved in 50% EtOH/H_2O (*v/v*) and formulated at different concentrations (0–100 μM). Sixty microliters of each test compound solution and 140 μL of DPPH solution were added to the test tube. The mixture was subsequently placed in a microplate shaker (Hangzhou Yuning Instrument Co., Ltd., China) and shaken at 37 °C for 20 min. Analysis was performed in triplicate for each sample. The UV absorbances of the compound-DPPH mixture and QR-DPPH mixture were measured at 517 nm and labeled A. The DPPH radical elimination rate was calculated according to Eq. (1). The dose–response curve plot between the inhibition rate and concentration was then analyzed via linear regression to derive the effective concentration of each sample needed to scavenge 50% of the DPPH (IC_{50} value) [20, 21]. The experiment was repeated three times.

$$\text{DPPH clearance (\%)} = \left(1 - \frac{A - A0}{A1}\right) \times 100\% \quad (1)$$

A0: Absorption of the blank group, anhydrous ethanol. A1: In the control group, 60 μL of 50% EtOH/H_2O (*v/v*) was mixed with 140 μL of DPPH solution.

Cell culture

HepG2 cells were supplemented with DMEM supplemented with 10% FBS, 100 U/mL penicillin and 100 mg/mL streptomycin [22]. The cells were kept in saturated air humidity containing 5% CO_2 at 310.15 K. During cell line metastasis, the cells were collected at a concentration of approximately 80% confluence and isolated with trypsin–EDTA solution (0.25% trypsin, 0.02% EDTA). The cells were selected and tested in the following experiments.

Cell viability assay

Cell viability was determined via MTT assays [23]. In brief, HepG2 cells were added to 96-well plates (0.5×10^4 cells/well) in DMEM supplemented with 10% FBS. After 12 h, the cells were separately treated with various concentrations of the test compound and QR for 20 h, followed by the addition of 10% MTT (5 mg/mL) and incubation for 4 h at 37 °C until the formazan crystals were completely dissolved in DMSO. The optical density at a wavelength of 490 nm was measured via a multimode detection platform, and the cell viability was calculated accordingly [24].

For the HepG2 cell injury model induced by H_2O_2, the cells were added to 96-well plates (0.5×10^4 cells/well). After 12 h of continuous cell culture, the supernatant in the 96-well plates was discarded, and different concentrations of the test compounds and QR were added for 20 h. Next, the cells were placed in 100 μL of H_2O_2 (800 μM) for 4 h, while the controls were treated with 100 μL of culture medium. Cell survival was determined by the MTT assay. An Olympus phase contrast microscope was used to capture the morphological features of the cells.

Determination of intercellular ROS

The cells were seeded in 6-well plates (1.5×10^5 cells/well). The protective group was separately incubated with each test compound and the QR solution at a concentration of 20 μM for 20 h [25]. Moreover, the normal control group was cultured in 100 μL of culture medium for 20 h. Both the injured group, the compound treatment group and the QR treatment group were incubated with H_2O_2 solution at a concentration of 800 μM for 4 h. Then, the medium was replaced with DMEM supplemented with 10 μM DCFH-DA solution and incubated for 30 min [26]. The supernatant from the medium was discarded again, and the cells were washed three times with PBS, which was previously refrigerated at 4 °C. The cells were subsequently detached into a single-cell suspension and detected via flow cytometry at an excitation wavelength (Ex) of 470/20 nm and an emission wavelength (Em) of 530/20 nm.

Statistical analyses

All the experiments were repeated three times, and the data are presented as the means ± standard deviations. Statistical analysis was performed via one-way ANOVA or Student's t test via SPSS version 18.0 statistical analysis software (SPSS, Chicago, IL, USA), with a *P*-value less than 0.05, indicating statistical significance.

Results and discussion

Enrichment of free radical inhibitors in the Fr2 sample

MeOH is widely used as a solvent for extraction because of its circularity and low toxicity. Approximately 65.0 g of crude extract was successfully extracted from 500.0 g of *S. tangutica* whole herb, with an extraction efficiency of approximately 13%. The crude extract was enriched with a large amount of chlorophyll, which led to a significant decrease in its solubilization and adsorption capacity in the stationary phase [27]. In the present study, the crude extract of *S. tangutica* was pretreated via two medium-pressure chromatographic columns. The dried extract–polyamide mixture was pretreated in a preparative liquid chromatography system via a medium–pressure column, an MCI GEL® CHP20P column. The connection schematic diagram of the system is displayed in Fig. 1A1. The sample loading column and the MCI GEL® CHP20P separation column are made of glass. The maximum pressure of the whole medium-pressure preparative liquid chromatography (MPLC) system was 2.5 MPa. The separation chromatogram of the crude sample is shown in Fig. 1A2. In this study, Fr2 (2.84 g) was used as a target sample to demonstrate target isolation of strong polarity galloyl glucosides.

In the screening of free radical inhibitors from complex compounds, online RPLC-HPLC is undoubtedly a fast, efficient and proven technique. In conventional HPLC analysis, suitable chromatographic separation conditions are the key to solving separation problems. Similarly, the selection of optimal chromatographic conditions is crucial for RPLC-DPPH analysis. In this study, the activity of free radical inhibitors of DPPH by online HPLC-DPPH was determined in combination with the optimized chromatographic separation conditions of the Fr2 (56.8 mg/mL) sample. A diagram and schematic diagram of the online HPLC-DPPH system are shown in Fig. 1B1. As shown in Fig. 1B2 and 1B3, the Fr2 samples were retained on the C18 column for between 5 and 25 min, and five major DPPH inhibitor chromatographic peaks were observed (negative peaks I–VI within the red dotted line in Fig. 1B correspond to the hearts).

The complexity (Fig. 1B2) of the *S. tangutica* Fr2 samples made the separation of free radical inhibitors difficult. Therefore, the target components need to be

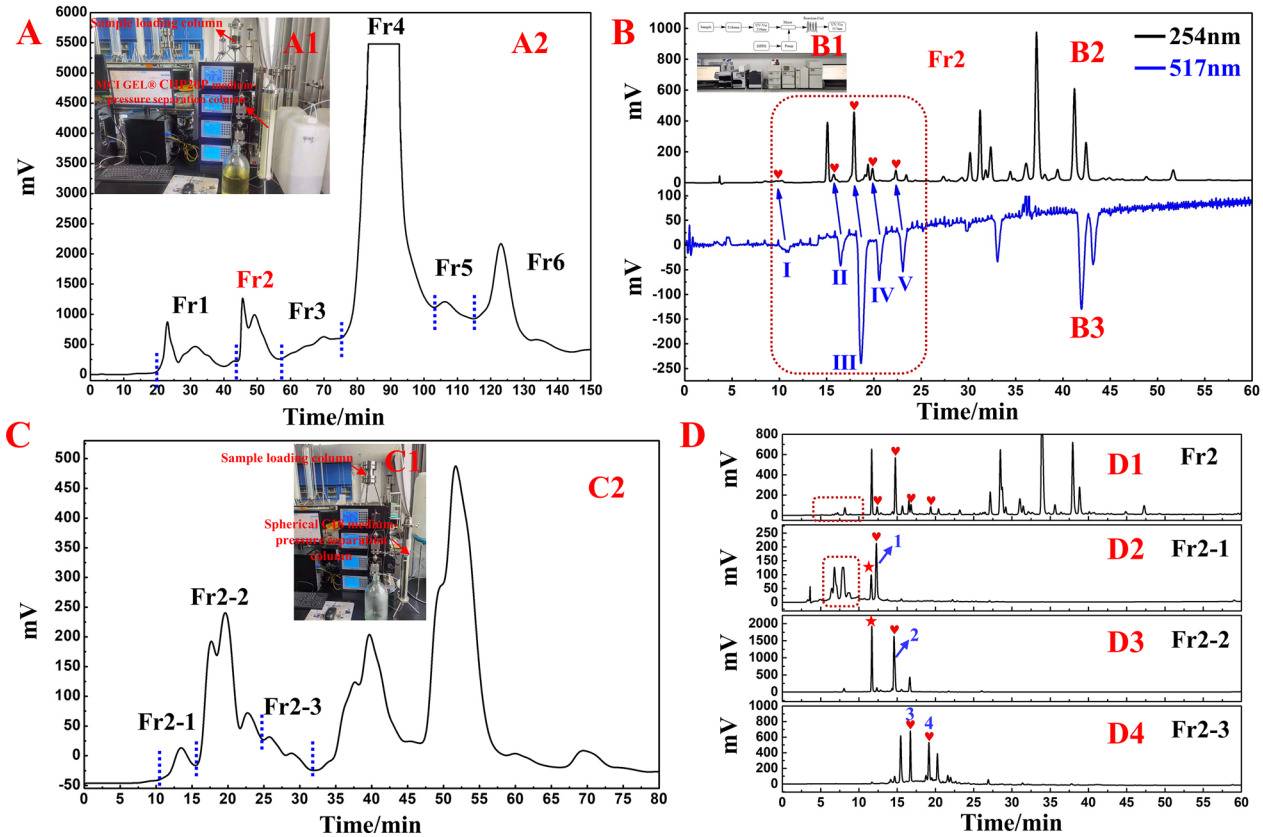

Fig. 1 **A** MCI GEL® CHP20P MPLC separation chromatogram of the *Saxifraga tangutica* crude sample. **B** DPPH activity scavenging chromatogram of the *Saxifraga tangutica* fraction Fr2 sample obtained via RPLC-DPPH. **C** Spherical C18 preparation chromatogram of the *Saxifraga tangutica* Fr2 sample. **D** HPLC chromatograms of the Fr2 and Fr2-1-Fr2-3 samples

enriched. According to the experimental conditions, the active ingredient had good retention performance for RPLC packing, and the Fr2 sample did not contain chlorophyll. To further improve the separation effect, a spherical C18 material with a large particle size (50 μm) was used to pretreat the sample. The pretreatment process was carried out by filling the medium–pressure column and placing it on a preparative liquid chromatography system. The chromatograms obtained from the experiments (Fig. 1C) revealed that the separation was very satisfactory and that the target fractions could be collected efficiently (hearts dashed box in Fig. 1C). Eventually, three fractions (Fr2-1 ~ Fr2-3) were separated via MPLC separations and acquired with a recovery of 42.4%. This result indicates that the experimental method is effective. The redissolved fractions Fr2-1, Fr2-2 and Fr2-3 were analyzed on a reversed-phase C18 column (ReproSil-Pur C18 AQ), and the results are shown in Fig. 1D. Upon careful observation of the analytical charts of the Fr2-1 to Fr2-3 components (hearts in Fig. 1D2–D4), four DPPH inhibitors were efficiently enriched in the *S. tangutica* Fr2 crude sample, as displayed in Fig. 1D. Additionally, peaks 1–4 (Fig. 1D2–D4) were attributed to the four microconstituents (Fig. 1D1) in the Fr2 sample. Notably, the microconstituents observed in the *S. tangutica* Fr2 sample (red dashed line, retention times between 5 and 12 min) were enriched and became macroconstituents in the Fr2-1 sample (Fig. 1D2), which was highly important for discovering more DPPH inhibitors from the *S. tangutica* Fr2 sample.

Target separation of free radical inhibitors and their active verification and structural identification

Starting with the chromatograms in Fig. 1D2–D4, the separation conditions on the same analytical column were further optimized to improve peak resolution and purification efficiency. Using online RPLC-DPPH devices and conditions optimized for fractions Fr2-1, Fr2-2 and Fr2-3, fraction Fr2-1 has three distinct peaks (peaks 5, 6, and 1 corresponding to negative DPPH I-II) (Fig. 2A1 and A2), a good resolution peak (peak 2 corresponding to a negative peak of DPPH III) was observed for fractions Fr2-2 (Fig. 2B1 and B2), and fraction Fr2-3 has two well-resolved peaks (peaks 3 and 4 corresponding to DPPH negative peaks IV and V) (Fig. 2C1 and C2). Fr2-1, Fr2-2 and Fr2-3 were prepared at a flow velocity of 19.0 mL/min via an RP-C18 preparative column (ReproSil-Pur C18 AQ, 20×250 mm), whereas the injection volumes were 1.0 mL, 2.5 mL and 2.0 mL for fractions Fr2-1, Fr2-2 and Fr2-3, respectively. Figure 2D1–D3 display the

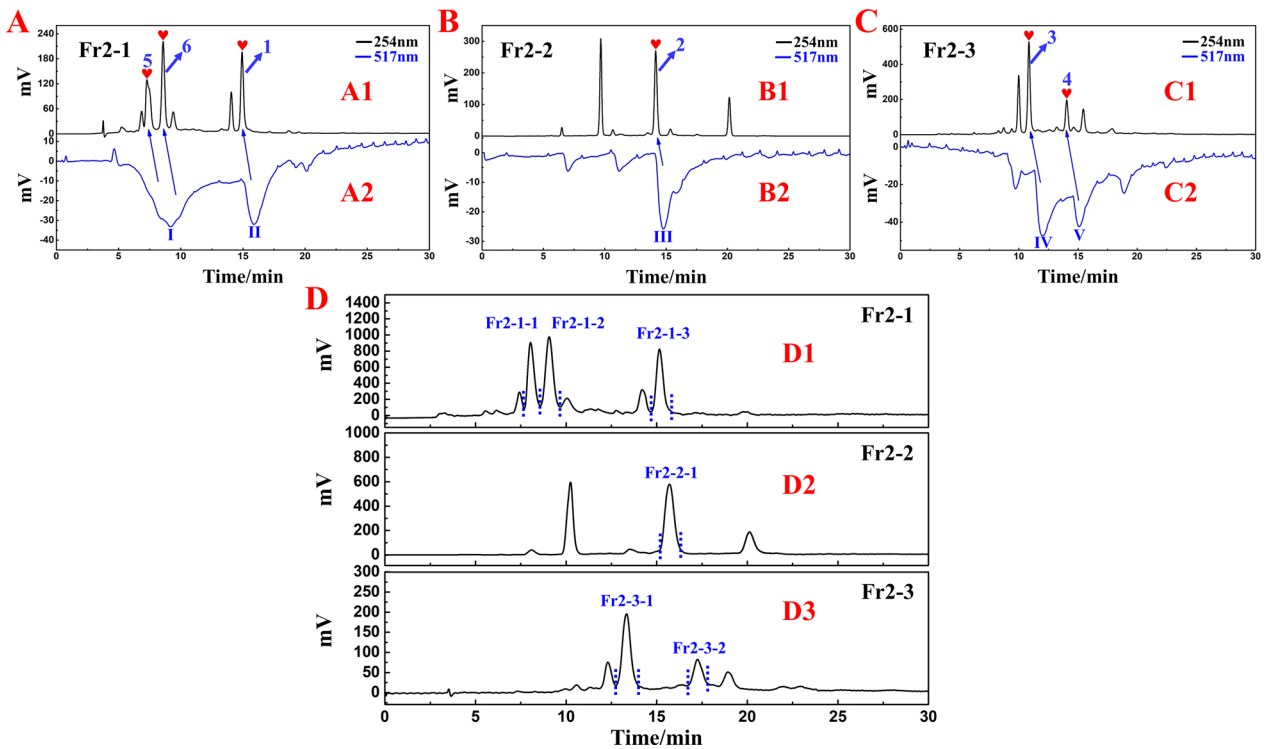

Fig. 2 **A** DPPH activity scavenging chromatogram of the Fr2-1 sample obtained via the RPLC-DPPH method. **B** DPPH activity scavenging chromatogram of the Fr2-2 sample obtained via the RPLC-DPPH method. **C** DPPH activity scavenging chromatogram of the Fr2-3 sample obtained via the RPLC-DPPH method. **D** Preparative chromatograms of the Fr2-1, Fr2-2, and Fr2-3 fractions

preparative chromatograms of fractions Fr2-1, Fr2-2 and Fr2-3.

A comparison of Figs. 2A–C and 3A–C revealed that the retention times of active chromatographic peaks 1–6 were almost the same on the preparative and analytical columns with the same stationary phase (ReproSil-Pur C18 AQ). Fractions Fr2-1, Fr2-2 and Fr2-3 were collected from fractions Fr2-1-1, Fr2-1-2, Fr2-1-3, Fr2-2-1, Fr2-3-1 and Fr2-3-2, respectively, after a number of preparation and separation processes, leading to 3.5 mg of Fr2-1-1, 4.2 mg of Fr2-1-2, 8.9 mg of Fr2-1-3, 133.9 mg of Fr2-2-1, 27.2 mg of Fr2-3-1 and 13.4 mg of Fr2-3-2. Interestingly, the prepared isolated DPPH inhibitors (fractions Fr2-1-1, Fr2-1-2 and Fr2-1-3, Fr2-3-1 and Fr2-3-2, Fig. 3A–C) presented a pair of observable chromatographic peaks, with the exception of Fr2-2-1 (Fig. 3B2), and all the DPPH inhibitors presented a molecular ion peak of 331 in negative ion mode (Figures S1F, S2F, S3C and S4F). On the basis of the above information, we speculated that fractions Fr2-1-1, Fr2-1-2 and Fr2-1-3, Fr2-3-1 and Fr2-3-2 were three pairs of natural tautomers that were combined. In addition, the activities of the isolated DPPH inhibitors, Fr2-1-1, Fr2-1-2/Fr2-1-3, Fr2-2-1, and Fr2-3-1/Fr2-3-2 were reassessed via an online HPLC-DPPH system, and the conditions were optimized on an RP-C18 column.

As demonstrated in Fig. 4A–D, all the isolated DPPH inhibitors, including tautomers (Fr2-1-1, Fr2-1-2/Fr2-1-3, Fr2-2-1 and Fr2-3-1/Fr2-3-2), could achieve baseline separation and had DPPH inhibitory activity. To characterize the specific structures of the isolated active compounds, ^{1}H-nuclear magnetic resonance (^{1}H NMR), ^{13}C-nuclear magnetic resonance (^{13}C NMR), heteronuclear single quantum coherence (HSQC), heteronuclear multiple bond correlation (HMBC), distortionless enhancement by polarization transfer (DEPT), and ESI–MS spectral data were obtained and compared with those of available studies. The NMR and ESI–MS data of fractions Fr2-1-1, Fr2-1-2/Fr2-1-3, Fr2-2-1, and Fr2-3-1/Fr2-3-2 matched the data for 3-*O*-Galloyl-α-D-glucose ⇌ 3-*O*-Galloyl-β-D-glucose [28], 2-*O*-Galloyl-α-D-glucose ⇌ 2-*O*-Galloyl-β-D-glucose [29], 1-*O*-Galloyl-β-D-glucose [30], and 6-*O*-Galloyl-α-D-glucose ⇌ 6-*O*-Galloyl-β-D-glucose [31], respectively (Fig. 5A). All the data are presented in full (Figures S1–S4).

Antioxidant activity of the isolated active compounds in vitro and their structure–activity relationships

DPPH free radicals are extensively utilized to measure the antioxidant scavenging ability of NPs [32]. To assess the antioxidant effects of the isolated compounds Fr2-1-1, Fr2-1-2/Fr2-1-3, Fr2-2-1, and Fr2-3-1/Fr2-3-2 in vitro, DPPH free radical scavenging experiments were performed. Additionally, quercetin (QR) was used as a positive control. Figure 5B shows that all four compounds and QR displayed strong antioxidant activity in a concentration-dependent manner (0–100 μM). When the concentration was 24 μM, the scavenging activities of Fr2-1-2/Fr2-1-3, Fr2-2-1, and Fr2-3-1/Fr2-3-2 were greater than 80%. However, the scavenging ability of Fr2-1-1 and QR (positive control) seemed slightly weaker. The IC_{50} values were 18.61 ± 3.55 μM, 17.14 ± 0.95 μM, 5.52 ± 0.32 μM, 7.22 ± 0.57 μM and 7.36 ± 0.25 μM for QR, Fr2-1-1, Fr2-1-2/Fr2-1-3, Fr2-2-1 and Fr2-3-1/Fr2-3-2, respectively.

Owing to their specific inhibition of phytochemicals in the liver, HepG2 cell lines are often used to detect their cytotoxicity and antiproliferative activity. This inhibition was associated with the production of ROS in cells [33]. H_2O_2 is a small molecule that easily crosses cell membranes and regulates cell growth and differentiation by activating oxidative phosphorylation in normal physiological environments [34]. In addition, H_2O_2 is a core component of the intracellular ROS that is formed during a variety of physiological and pathological processes [35]. Thus, to ascertain the oxidative protective properties of the isolated compounds, an H_2O_2-induced oxidative

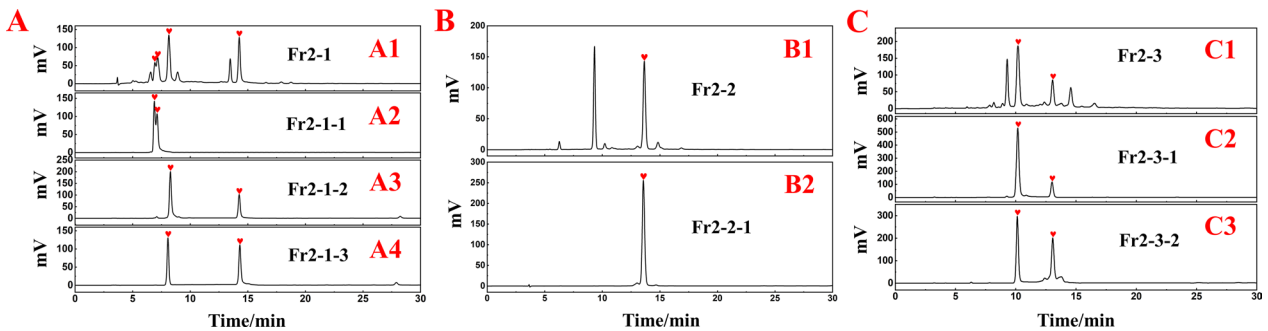

Fig. 3 **A** Analytical chromatograms of the Fr2-1, Fr2-1-1, Fr2-1-2, and Fr2-1-3 samples. **B** Analytical chromatograms of the Fr2-2 and Fr2-2–1 samples. **C** Analytical chromatograms of the Fr2-3, Fr2-3-1, and Fr2-3-2 samples

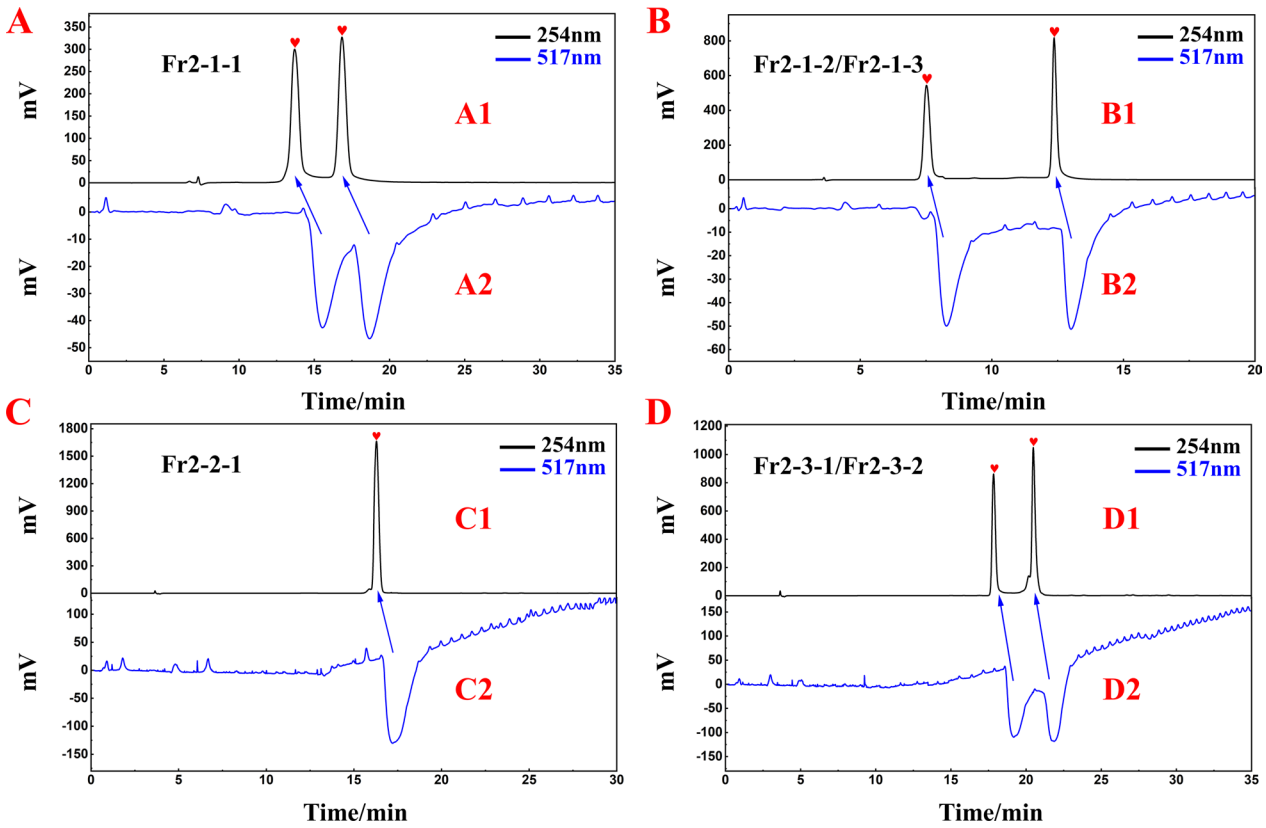

Fig. 4 **A** DPPH activity scavenging chromatogram of the *Saxifraga tangutica* fraction Fr2-1–1 obtained via RPLC-DPPH. **B** DPPH activity scavenging chromatogram of the *Saxifraga tangutica* fraction Fr2-1-2/Fr2-1-3 sample obtained via RPLC-DPPH. **C** DPPH activity scavenging chromatogram of the *Saxifraga tangutica* fraction Fr2-2-1 sample via the RPLC-DPPH method. **D** DPPH activity scavenging chromatogram of the *Saxifraga tangutica* fraction Fr2-3-1/Fr2-3-2 sample obtained via RPLC-DPPH

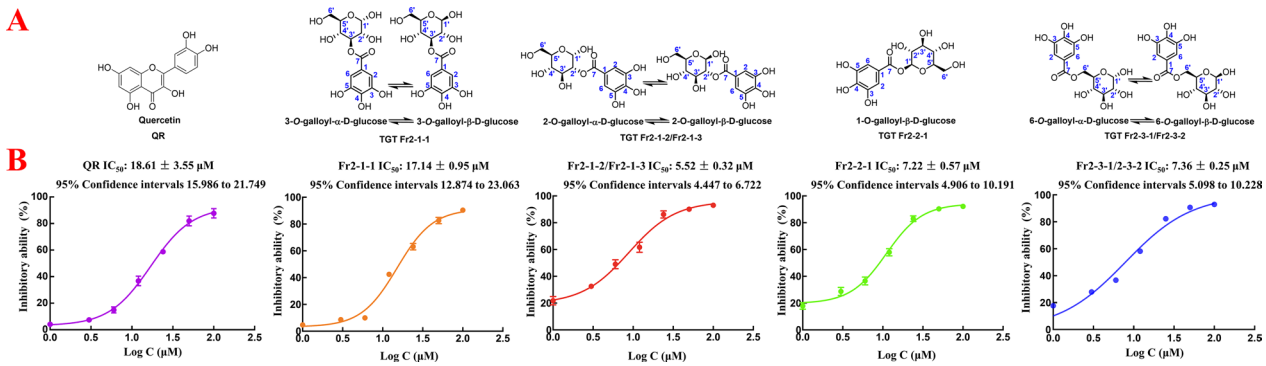

Fig. 5 **A** The chemical structural formulae of quercetin, Fr2-1-1, Fr2-1-2/2-1-3, Fr2-2-1 and Fr2-3-1/Fr2-3-2. **B** DPPH scavenging activities of quercetin, Fr2-1-1, Fr2-1-2/2-1-3, Fr2-2-1 and Fr2-3-1/Fr2-3-2

damage model in HepG2 cells was employed. As shown in Fig. 6, HepG2 cell viability was significantly affected by treatment with 800 μM H_2O_2 for 4 h. In addition, phase contrast microscopy was used to observe the morphological changes in the cells. In the groups treated with the *S. tangutica* fractions and QR, both the cell viability and the cell morphology improved to various degrees. Except for the Fr2-1-1 group and QR group, the cell viability of the other three treatment groups (Fr2-1-2/Fr2-1-3, Fr2-2-1 and Fr2-3-1/Fr2-3-2) significantly increased in a concentration-dependent manner ($P < 0.05$). Compared with those of the H_2O_2 group, the cell proliferation

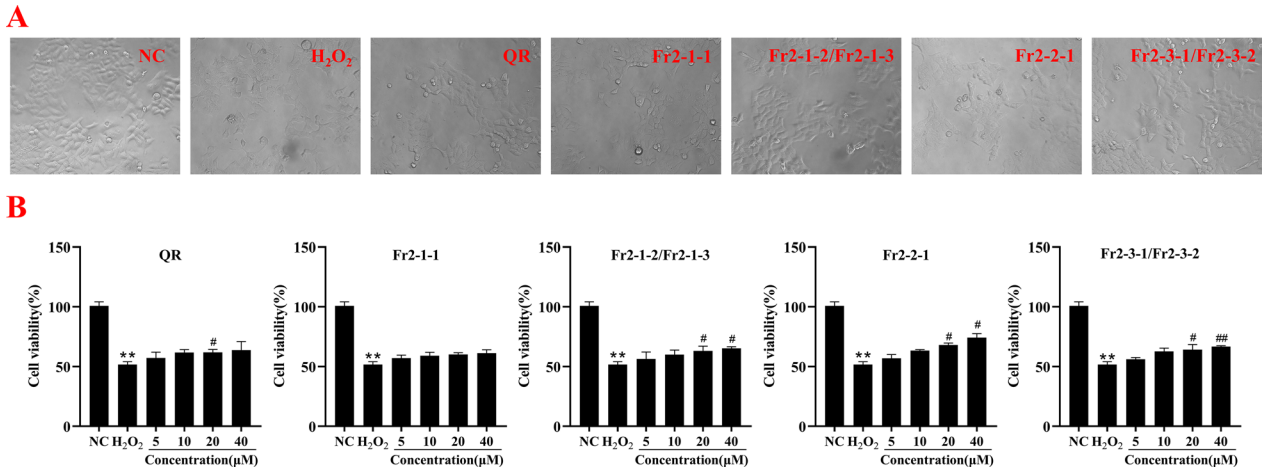

Fig. 6 Effects of the *Saxifraga tangutica* fractions (Fr2-1-1, Fr2-1-2/2-1-3, Fr2-2-1 and Fr2-3-1/Fr2-3-2) and quercetin on the morphological changes (**A**) and viability (**B**) of H_2O_2-damaged HepG2 cells. ($^{**}P<0.01$, vs the normal control groups. $^{\#}P<0.05$, $^{\#\#}P<0.01$ vs the H_2O_2 groups)

rates of these three groups at 40 μM were increased by 26.05 ± 2.58% (Fr2-1-2/Fr2-1-3), 43.41 ± 6.55% (Fr2-2-1) and 28.78 ± 1.59% (Fr2-3-1/Fr2-3-2). These results suggest that isolated DPPH inhibitors from *S. tangutica* could effectively protect HepG2 cells from oxidative stress damage caused by H_2O_2.

ROS are important intermediates in the oxidative metabolism of organisms. They are involved in many biochemical reactions and can cause many diseases [36]. Increased concentrations of free Ca^{2+} in cells due to excess ROS accumulation further trigger mitochondrial dysfunction, which may eventually lead to cell death [37]. HepG2 cells treated with H_2O_2 presented significant increases in intracellular ROS levels [38–40]. Therefore, we tested the production of intracellular ROS via flow cytometry. The results in Fig. 7 demonstrate that the ROS levels were significantly elevated with H_2O_2 treatment ($P<0.01$) and were 2 times greater than those in the normal group, suggesting that the H_2O_2-treated HepG2 cells experienced oxidative stress injury. Treatment with 40 μM *S. tangutica* fractions significantly decreased intracellular ROS production in HepG2 cells ($P<0.05$).

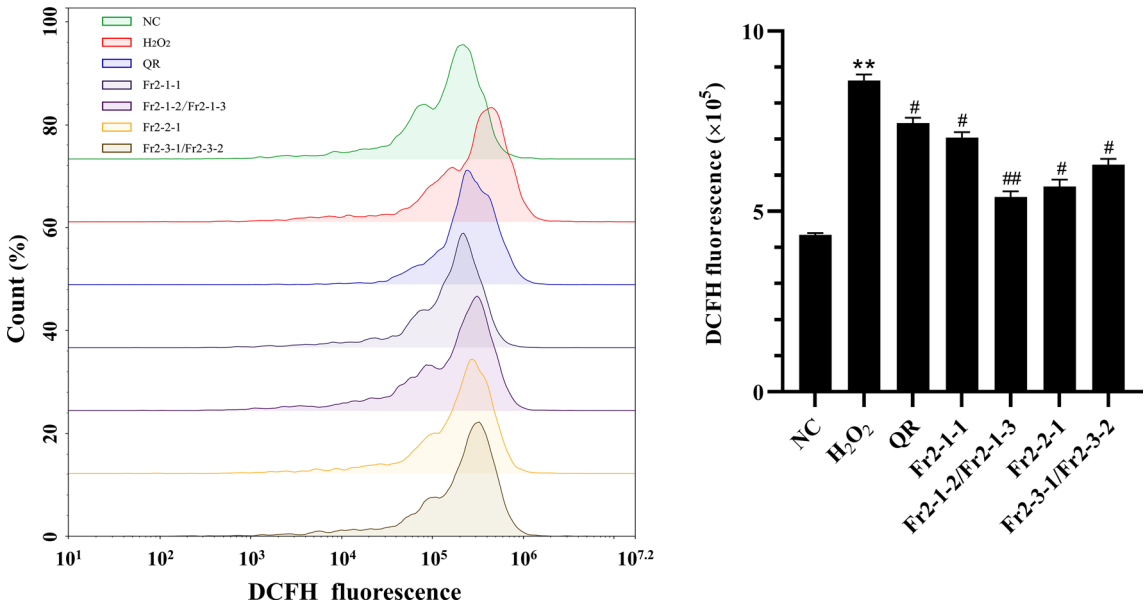

Fig. 7 Effects of the *Saxifraga tangutica* fractions (Fr2-1–1, Fr2-1-2/2-1-3, Fr2-2-1 and Fr2-3-1/Fr2-3-2) and quercetin on the generation of intracellular ROS in H_2O_2-damaged HepG2 cells. ($^{**}P<0.01$, vs the normal control groups. $^{\#}P<0.05$, $^{\#\#}P<0.01$ vs the H_2O_2 groups)

Compared with those in the injury group, the ROS levels in HepG2 cells pretreated with compounds and QR decreased by 13.69 ± 3.64% (QR group), 18.35 ± 2.66% (Fr2-1-1 group), 37.48 ± 4.34% (Fr2-1-2/Fr2-1-3 group), 34.14 ± 6.08% (Fr2-2-1 group), and 27.02 ± 0.62% (Fr2-3-1/Fr2-3-2 group). In the Fr2-1-2/Fr2-1-3 groups, which presented the most dramatic decrease, the ROS levels decreased to approximately 124.15 ± 4.16% of those in the normal control group. Overall, among the four compounds and QR, the ability of QR was relatively weak. These results indicate that four galloyl glucoside tautomers (Fr2-1-1, Fr2-1-2/Fr2-1-3, Fr2-2-1, and Fr2-3-1/Fr2-3-2) have good ROS scavenging ability in vitro and inhibit the oxidative damage of ROS to cell membranes and intracellular substances, which in turn exerts antioxidant effects.

Conclusions

In summary, an efficient method based on two-step MPLC, online RPLC-DPPH analysis and one-step HPLC was used to enrich, screen and isolate the galloyl glucoside isomers of DPPH inhibitors in this study. Four galloyl glucoside tautomers (Fr2-1-1, Fr2-1-2/Fr2-1-3, Fr2-2-1, and Fr2-3-1/Fr2-3-2) were isolated and identified for the first time from *Saxifraga tangutica* (*S. tangutica*) extract. Free radical scavenging assays in vitro revealed that compounds Fr2-1-1 (IC_{50}: 17.14 ± 0.95 μM), Fr2-1-2/Fr2-1-3 (IC_{50}: 5.52 ± 0.32 μM), Fr2-2-1 (IC_{50}: 7.22 ± 0.57 μM), and Fr2-3-1/Fr2-3-2 (IC_{50}: 7.36 ± 0.25 μM) possessed strong free radical scavenging ability and were superior to quercetin. To further elucidate the conformational relationship between galloyl glucoside tautomers with different structures and antioxidant activity, four compounds isolated from *S. tangutica* were found to possess certain inhibitory activities against injury in HepG2 cells by evaluating H_2O_2-induced ROS levels ($P < 0.05$). Among them, the protective effect of 2-*O*-galloyl-α-D-glucose ⇌ 2-*O*-galloyl-β-D-glucose (Fr2-1-2/Fr2-1-3) on oxidative stress injury in HepG2 cells was extremely significant ($P < 0.01$). These findings provide new ideas for its structural modification and mechanism of action. Future studies need to focus on the hepatoprotective activity of *S. tangutica* extract and elucidate its molecular mechanism. Additionally, the method of MPLC combined with on-line HPLC-DPPH for rapid enrichment, screening, and isolation of antioxidants in this paper is also applicable to the isolation of antioxidants from other natural products (NPs), providing new insights into the isolation of NPs.

Abbreviations

Saxifraga tangutica	*S. tangutica*
ROS	Reactive oxygen species
RNS	Reactive nitrogen species
NPs	Natural products
HPLC-DPPH	High-performance liquid chromatography-1,1-diphenyl-2-picrylhydrazyl
ESI–MS	Electrospray ionization-mass spectrometry
QR	Quercetin
RPLC	Reversed-phase liquid chromatography
DMEM	Dulbecco's modified Eagle's medium
FBS	Fetal bovine serum
MTT	3-(4,5-Dimethylthiazol-2-thiazolyl)-2,5-diphenyltetrazolium bromide
DCFH-DA	2,7-Dichlorodi-hydrofluorescein diacetate
DMSO	Dimethylsulfoxide
MPLC	Medium-pressure preparative liquid chromatography
Ex	Excitation wavelength
Em	Emission wavelength
^{1}H NMR	^{1}H-nuclear magnetic resonance
^{13}C NMR	^{13}C-nuclear magnetic resonance
HMBC	Heteronuclear multiple bond correlation
HSQC	Heteronuclear single quantum coherence
DEPT	Distortionless enhancement by polarization transfer

Supplementary Information

The online version contains supplementary material available at https://doi.org/10.1186/s13065-024-01330-z.

Supplementary Material 1

Acknowledgements

The authors thank the funding support of Young Scholars in Western China, Chinese Academy of Sciences.

Author contributions

TYY performed part of the chemical experiments, data processing and writing; CM and ZJ performed the biological experiments; WQL fulfilled data processing, funding support and supervision; DJ and LG provided design of experiments, funding support, structural identification and supervision; AMAEA performed modification of paper and editing. All the authors read and approved the final manuscript.

Funding

This study was implemented in favor of the National Natural Science Foundation of China (Grant No: 32470429).

Availability of data and materials

All data generated or analyzed during this study are included in this published article. The data are available upon reasonable request from the corresponding authors.

Declarations

Ethics approval and consent to participate

Not applicable.

Consent for publication

Not applicable.

Competing interests

The authors declare no competing interests.

Author details

[1]Qinghai Provincial Key Laboratory of Tibetan Medicine Research, Key Laboratory of Tibetan Medicine Research, Northwest Institute of Plateau Biology, Chinese Academy of Sciences, Xining 810001, Qinghai, People's Republic of China. [2]Center for Mitochondria and Healthy Aging, College of Life Sciences, Yantai University, Yantai 264005, China. [3]Department of Pharmacology, Faculty of Veterinary Medicine, Cairo University, Giza 12211, Egypt. [4]Department of Medical Pharmacology, Faculty of Medicine, Atatürk University, Erzurum 25240, Turkey.

Received: 13 November 2023 Accepted: 25 October 2024
Published online: 08 November 2024

References

1. Zhou X, Zeng WN, Rong S, Lv H, Chen YH, Mao YH, Tan WL, Li H. Alendronate-modified nanoceria with multiantioxidant enzyme-mimetic activity for reactive oxygen species/reactive nitrogen species scavenging from cigarette smoke. ACS Appl Mater Interfaces. 2021;13(40):47394–406.
2. Hughes MCB, Williams GM, Pageon H, Fourtanier A, Green AC. Dietary antioxidant capacity and skin photoaging: a 15-year longitudinal study. J Invest Dermatol. 2021;141(4):1111–8.
3. Antalis E, Oikonomopoulou Z, Kottaridi C, Kossyvakis A, Spathis A, Magkana M, Katsouli A, Tsagris V, Papaevangelou V, et al. Mixed viral infections of the respiratory tract; an epidemiological study during consecutive winter seasons. J Med Virol. 2018;90(4):663–70.
4. Ornatowski W, Lu Q, Yegambaram M, Garcia AE, Zemskov EA, Maltepe E, Fineman JR, Wang T, Black SM. Complex interplay between autophagy and oxidative stress in the development of pulmonary disease. Redox Biol. 2020;36: 101679.
5. Akaike T, Ando M, Oda T, Doi T, Ijiri S, Araki S, Maeda H. Dependence on O_2- generation by xanthine oxidase of pathogenesis of influenza virus infection in mice. J Clin Invest. 1990;85(3):739–45.
6. Chen Y, Hu K, Bu HR, Si ZH, Sun HH, Chen LM, Liu H, Xie H, Zhao P, Yang L, et al. Probucol protects circulating endothelial progenitor cells from ambient PM2.5 damage via inhibition of reactive oxygen species and inflammatory cytokine production in vivo. Exp Ther Med. 2018;16(6):4322–8.
7. Chen QQ, Liu WL, Sun X, Liu KJ, Pan R. Endogenous reactive oxygen species and nitric oxide have opposite roles in regulating HIF-1alpha expression in hypoxic astrocytes. Biophys Rep. 2021;7(3):239–49.
8. Hu JH, An BJ, Pan TT, Li ZCX, Huang L, Li XS. Design, synthesis, and biological evaluation of histone deacetylase inhibitors possessing glutathione peroxidase-like and antioxidant activities against Alzheimer's disease. Bioorg Med Chem. 2018;26(21):5718–29.
9. Yousefian M, Shakour N, Hosseinzadeh H, Hayes AW, Hadizadeh F, Karimi G. The natural phenolic compounds as modulators of NADPH oxidases in hypertension. Phytomedicine. 2019;55:200–13.
10. Mangmool S, Kunpukpong I, Kitphati W, Anantachoke N. Antioxidant and anticholinesterase activities of extracts and phytochemicals of *Syzygium antisepticum* leaves. Molecules. 2021;26(11):3295.
11. Rebelo D, Correia AT, Nunes B. Acute and chronic effects of environmental realistic concentrations of simvastatin in *danio rerio*: evidences of oxidative alterations and endocrine disruptive activity. Environ Toxicol Pharmacol. 2021;81: 103522.
12. Cui W, Zeng QY. Antitumor effect of flavonoids from *Saxifraga tangutica* Engl. on H22 hepatoma mice. Chin Vet Sci. 2020;50(2):262–8.
13. Dang J, Jiao LJ, Wang WD, Pei JJ, Tao YD, Shao Y, Mei LJ, Wang QL, Zhang L. Chemotaxonomic importance of diarylheptanoids and phenylpropanoids in *Saxifraga tangutica* (Saxifragaceae). Biochem Syst Ecol. 2017;72:29–31.
14. Dang J, Zhang L, Wang QL, Mei LJ, Yue HL, Liu ZG, Shao Y, Gao QB, Tao YD. Target separation of flavonoids from *Saxifraga tangutica* using two-dimensional hydrophilic interaction chromatography/reversed-phase liquid chromatography. J Sep Sci. 2018;41(24):4419–29.
15. Dang J, Wang Q, Wang QL, Yuan C, Li G, Ji TF. Preparative isolation of antioxidative gallic acid derivatives from *Saxifraga tangutica* using a class separation method based on medium-pressure liquid chromatography and reversed-phase liquid chromatography. J Sep Sci. 2021;44(20):3734–46.
16. Dang J, Du YR, Wang Q, Dawa Y, Chen CB, Wang QL, Ma JB, Tao YD. Preparative isolation of arylbutanoid-type phenol [(-)-rhododendrin] with peak tailing on conventional C18 column using middle chromatogram isolated gel column coupled with reversed-phase liquid chromatography. J Sep Sci. 2020;43(16):3233–41.
17. Zhang QW, Lin LG, Ye WC. Techniques for extraction and isolation of natural products: a comprehensive review. Chinese Medicine. 2022;13:20.
18. Dar AA, Sangwan PL, Kumar A. Chromatography: an important tool for drug discovery. J Sep Sci. 2019;43(1):105–19.
19. Dawa YZ, Du YR, Wang Q, Chen CB, Zou DL, Qi DS, Ma JB, Dang J. Targeted isolation of 1,1-diphenyl-2-picrylhydrazyl inhibitors from *Saxifraga atrata* using medium- and high- pressure liquid chromatography combined with online high performance liquid chromatography-1,1-diphenyl-2-picrylhydrazyl detection. J Chromatogr A. 2021;1635: 461690.
20. Feng XJ, Bie NN, Li JY, Zhang ML, Feng YH, Ding TT, Zhao Y, Wang CL. Effect of *in vitro* simulated gastrointestinal digestion on the antioxidant activity, molecular weight, and microstructure of polysaccharides from Chinese yam. Int J Biol Macromol. 2022;207(15):873–82.
21. Tunnisa F, Faridah DN, Afriyanti A, Rosalina D, Syabana MA, Darmawan N, Yuliana ND. Antioxidant and antidiabetic compounds identification in several Indonesian underutilized *Zingiberaceae* spices using SPME-GC/MS-based volatilomics and in silico methods. Food Chem X. 2022;14: 100285.
22. Guo JX, Gao Y, Cao XL, Zhang J, Chen W. Cholesterol-lowing effect of taurine in HepG2 cell. Lipids Health Dis. 2017;38(6):350–3.
23. Ma JG, Feng YY, Jiang SY, Li XY. Altered cellular metabolism of HepG2 cells caused by microcystin-LR. Environ Pollut. 2017;225:610–9.
24. Yang LS, Ji WW, Zhong H, Wang LY, Zhu XL, Zhu J. Anti-tumor effect of volatile oil from *Houttuynia cordata* Thunb. on HepG2 cells and HepG2 tumor-bearing mice. RSC Adv. 2019;9(54):31517–26.
25. Long XS, Hu X, Pan C, Xiang H, Chen SJ, Qi B, Liu SC, Yang XQ. Antioxidant activity of *Gracilaria lemaneiformis* polysaccharide degradation based on Nrf-2/Keap-1 signaling pathway in HepG2 cells with oxidative stress induced by H_2O_2. Mar Drugs. 2022;20(9):545.
26. Xu JJ, Zhang YW, Ren GF, Yang RG, Chen JF, Xiang XJ, Qin H, Chen JH. Inhibitory effect of delphinidin on oxidative stress induced by H_2O_2 in HepG2 cells. Oxid Med Cell Longev. 2020;2020:4694760.
27. Petibon F, Wiesenberg GLB. Characterization of complex photosynthetic pigment profiles in European deciduous tree leaves by sequential extraction and reversed-phase high-performance liquid chromatography. Front Plant Sci. 2022;13: 957606.
28. Kandil FE, El-Sayed NH, Micheal HN, Ishak MS, Mabry TJ. Gallotannins and flavonoids from *Haematoxylon campechianum*. Phytochemistry. 1996;42(4):1243–5.
29. Pineda-Hidalgo KV, Vega-Alvarez E, Vega-Alvarez A, Salazar-Salas NY, Juárez-Barraza CI, López-Valenzuela JA. Chilling injury tolerance induced by quarantine hot water treatment in mango fruit is associated with an increase in the synthesis of gallotannins in the pulp. J Food Meas Charact. 2023;17(4):3295–308.
30. Tahara K, Nishiguchi M, Frolov A, Mittasch J, Milkowski C. Identification of UDP glucosyltransferases from the aluminum-resistant tree *Eucalyptus camaldulensis* forming β-glucogallin, the precursor of hydrolyzable tannins. Phytochemistry. 2018;152:154–61.
31. Yakubu OF, Adebayo AH, Dokunmu TM, Zhang YJ, Iweala EEJ. Cytotoxic effects of compounds isolated from *Ricinodendron heudelotii*. Molecules. 2019;24(1):145.
32. Martinez-Morales F, Alonso-Castro AJ, Zapata-Morales JR, Carranza-Alvarez C, Aragon-Martinez OH. Use of standardized units for a correct interpretation of IC_{50} values obtained from the inhibition of the DPPH radical by natural antioxidants. Chem Pap. 2020;74(10):3325–34.
33. Ma BT, Wang XB, Zhang R, Niu S, Rong ZH, Ni L, Di X, Han Q, Liu CW. Cigarette smoke extract stimulates PCSK9 production in HepG2 cells via ROS/NF-κB signaling. Mol Med Rep. 2021;23(5):331.
34. Chen K, Lu YW, Liu CY, Zhang LM, Fang ZY, Yu GR. Morroniside prevents H_2O_2 or $A\beta_{1-42}$-induced apoptosis via attenuating JNK and p38 MAPK phosphorylation. Eur J Pharmacol. 2018;834:295–304.
35. Miller IP, Pavlovic I, Poljsak B, Suput D, Milisav I. Beneficial role of ROS in Cell survival: moderate increases in H_2O_2 production induced by hepatocyte isolation mediate stress adaptation and enhanced survival. Antioxidants. 2019;8(10):434.
36. Juan CA, de la Lastra JMP, Plou FJ, Pérez-Lebeña E. The chemistry of reactive oxygen species (ROS) revisited: outlining their role in biological macromolecules (DNA, lipids and proteins) and induced pathologies. Int J Mol Sci. 2021;22(9):4642.
37. Shao FY, Han JY, Tian ZY, Wang Z, Liu SQ, Wu YF. Synergistic ROS generation and directional overloading of endogenous calcium induce mitochondrial dysfunction in living cells. Biomaterials. 2023;301: 122284.
38. Zhang MJ, Zhang GS, Meng XX, Wang XX, Xie J, Wang SS, Wang B, et al. Reduction of the oxidative damage to H_2O_2-induced HepG2 cells via the

Nrf2 signalling pathway by plant flavonoids Quercetin and Hyperoside. Food Sci Hum Wellness. 2024;13:1864–76.
39. Hu YM, Lu SZ, Li YS, Wang H, Shi Y, Zhang L, Tu ZC. Protective effect of antioxidant peptides from grass carp scale gelatin on the H_2O_2-mediated oxidative injured HepG2 cells. Food Chem. 2022;373: 131539.
40. Zhang A, Cui L, Tu XB, Liang Y, Wang L, Sun YY, Kang X, Wu Z. Peptides derived from casein hydrolyzed by Lactobacillus: screening and antioxidant properties in H_2O_2-induced HepG2 cells model. J Funct Food. 2024;117: 106221.

Publisher's Note